

## ADSORPTION OF NITRILOTRIACETATE (NTA), Co AND CoNTA BY GIBBSITE

D. C. GIRVIN,<sup>1</sup> P. L. GASSMAN<sup>1</sup> AND H. BOLTON, Jr.<sup>2</sup>

<sup>1</sup> Interfacial Geochemistry Group, Pacific Northwest National Laboratory, PO Box 999, MSIN: K3-61, Richland, Washington 99352

<sup>2</sup> Environmental Microbiology Group, Pacific Northwest National Laboratory, Richland, Washington 99352

**Abstract**—Adsorption of  $\text{Co}^{2+}$ , nitrilotriacetic acid (NTA) and equal-molar  $\text{Co}^{2+}$  and NTA by a low surface area (LSA) commercial gibbsite ( $3.5 \text{ m}^2 \text{ g}^{-1}$ ) was investigated in batch as a function of pH (4.5 to 10.5), adsorbate ( $0.5$  to  $10 \mu\text{M}$ ) and adsorbent ( $0.5$  to  $75 \text{ g L}^{-1}$ ) concentrations and ionic strength ( $0.01$  to  $1 \text{ M NaClO}_4$ ). The adsorption of  $\text{Co}^{2+}$  (Co-only) and the acid form of NTA (NTA-only) by gibbsite in  $0.01 \text{ M NaClO}_4$  exhibit cation-like and anion-like adsorption edges, respectively. For the equal-molar CoNTA chelate, Co and NTA adsorption edges were similar but not identical to the Co-only and NTA-only edges. Differences suggest the existence of a ternary CoNTA surface complex with the Co in the intact chelate coordinated to surface hydroxyls. NTA-only adsorption was insensitive to ionic strength variation, indicating weak electrostatic contributions to surface coordination reactions. This is consistent with the formation of inner-sphere surface NTA complexes and ligand exchange reactions in which monodentate, bidentate and binuclear NTA surface complexes form. Cobalt adsorption increases (edge shifts to lower pH by 1 pH unit) on LSA gibbsite as ionic strength increases from  $0.01$  to  $1 \text{ M NaClO}_4$ . For the same ionic strength change, a similar shift in the Co-only edge was observed for another commercial gibbsite ( $16.8 \text{ m}^2 \text{ g}^{-1}$ ); however, no change was observed for  $\delta\text{-Al}_2\text{O}_3$ . Ionic strength shifts in  $\text{Co}^{2+}$  adsorption by gibbsite were described as an outer-sphere  $\text{CoOH}^+$  surface complex using the triple-layer model. Results suggest that, at waste disposal sites where  $^{60}\text{Co}$  and NTA have been co-disposed, NTA will not promote ligand-like adsorption of Co for acid conditions, but will reduce cation-like adsorption for basic conditions. Thus, where gibbsite is the dominant mineral sorbent, NTA will not alter  $^{60}\text{Co}$  mobility in acidic pore waters and groundwaters; however, NTA could enhance  $^{60}\text{Co}$  mobility where alkaline conditions prevail, unless microbial degradation of the NTA occurs.

**Key Words**— $\delta\text{-Al}_2\text{O}_3$ , Adsorption, Chelate, Cobalt, Desorption, Gibbsite ( $\alpha\text{-Al}(\text{OH})_3$ ), Nitrilotriacetic Acid (NTA).

### INTRODUCTION

Aminopolycarboxylic chelating agents, such as nitrilotriacetic acid (NTA) and ethylenediaminetetraacetic acid (EDTA), have been extensively used in nuclear waste reprocessing to concentrate fission products and actinides from waste streams and to remove fission products and actinides from contaminated equipment and reactor cooling systems (Ayers 1970; Piciulo et al. 1986). The resulting chelate-radionuclide mixtures have been co-disposed at Department of Energy (DOE) waste disposal sites (Means and Alexander 1981; Toste, Lucke et al. 1987; Toste, Pahl et al. 1987; Riley et al. 1992). Synthetic chelating agents form strong water-soluble complexes with cationic radionuclides and, depending on environmental conditions, may alter the adsorption behavior of these radionuclides and thus facilitate their migration in soil pore waters and groundwaters at or near waste disposal sites. EDTA has been implicated in the enhanced migration of  $^{60}\text{Co}$  at several waste sites (Means et al. 1978; Olsen et al. 1986).

The influence of NTA and EDTA chelates upon transition metal adsorption by naturally occurring Fe, Al and Si oxide adsorbents depends upon multiple equilibria among the metal, the chelate and the solid.

These equilibria are affected by the individual adsorption constants of the metal and chelate for the particular solid, the aqueous stability constant of the metal-chelate complex and the stability constant between the chelate and the structural metal ions of the Fe and Al oxides. The pH-dependent surface charge of the hydrated oxide, as characterized by the point of zero charge ( $\text{pH}_{\text{pzc}}$ ), also influences chelate adsorption in either the free acid form or as a metal chelate.

For  $\alpha\text{-SiO}_2$  and silica-gel, with  $\text{pH}_{\text{pzc}}$  values in the range 2 to 3, no evidence of ligand-like adsorption of the chelate or the metal chelate has been observed for equal molar Pb-EDTA and Cu-EDTA (Vuceta 1976), Cu-EDTA (Bourg and Schindler 1979), Ni-EDTA (Bowers 1982) and Co-NTA (Osaki et al. 1990). As the chelate-to-metal ratio was increased in these studies, the cation-like adsorption decreased, because the solution chelate competed more effectively with the solid for the metal. The terms “cation-like” and “ligand-like” adsorption refer to the increase in adsorption that occurs with increasing and decreasing pH, respectively.

For high  $\text{pH}_{\text{pzc}}$  oxides such as Al and Fe oxides ( $8 < \text{pH}_{\text{pzc}} < 9.5$ ), metal adsorption in chelate-metal mixtures could be cation-like, ligand-like or a combi-

nation of the two depending on solution pH, metal-to-chelate ratio and solid-to-adsorbate ratio. Few studies of NTA or EDTA adsorption by Fe oxides have been performed. As expected, ligand-like adsorption occurred for the free acid (anion) form of NTA or EDTA in suspensions of crystalline Fe oxides ( $8.5 < \text{pH}_{\text{pzc}} < 9.3$ ) (Chang et al. 1983). Recent investigations of Co(II)EDTA adsorption on Fe-coated sands (Szecsody et al. 1994) and by Fe and Al oxide-dominated fluvial sediments (Zachara et al. 1994) showed that Co(II) adsorption in the presence of equal molar EDTA was ligand-like for  $\text{pH} > 7$ . However, for most materials below  $\text{pH} < 7$ , competition for the EDTA between Fe or Al ( $\text{H}^+$  promoted dissolution of solids) and Co(II) resulted in the dissociation of the Co(II)EDTA complex. Thus, for  $\text{pH} < 7$ , Co adsorption decreased with decreasing pH and was not strictly ligand-like. A similar pattern of adsorption on  $\delta\text{-Al}_2\text{O}_3$  was observed for equal molar Co(II)EDTA for pH 5 to 9.5 over a wide range of sorbate concentrations and solid-to-sorbate ratios (Girvin et al. 1993). Metal adsorption in equal-molar Cd-, Cu-, Ni-, Pb- and Zn-EDTA suspensions of  $\delta\text{-Al}_2\text{O}_3$  ( $\text{pH}_{\text{pzc}} = 9.2$ ), was ligand-like for Ni and Cu and mixed cation-ligand-like for Cd, Pb and Zn (Bowers and Huang 1986). In equal molar Cu-, Ni-, Pb-, Zn- and Cd-NTA suspensions of  $\delta\text{-Al}_2\text{O}_3$ , only Cu exhibited mixed cation- and ligand-like metal adsorption (Elliott 1979; Elliott and Huang 1979). For the other metals, cation-like adsorption dominated but was suppressed by the NTA; no ligand-like adsorption occurred. Studies on the adsorption NTA, EDTA and their metal chelates by gibbsite have not appeared in the literature.

This paper describes the adsorption of Co, NTA and equal molar CoNTA by gibbsite ( $\text{pH}_{\text{pzc}} \approx 11$ ) as a function of pH, ionic strength and adsorbate concentrations. Gibbsite was chosen for study because it is common in many soils (Hsu 1989), it is possibly the most significant aluminum-bearing oxide in both soils and sediments (Davis and Hem 1989) and it supports both anion and cation adsorption. Adsorption reactions and surface coordination schemes are proposed to qualitatively describe the observed adsorption behavior of NTA and CoNTA. These results suggest how NTA can modify  $^{60}\text{Co}$  adsorption and migration in soil pore and groundwaters where gibbsite is an important mineral sorbent.

## MATERIALS AND METHODS

### Preparation and Characterization of Adsorbents

Two commercial gibbsite solids were used: a low surface area gibbsite ( $3.5 \text{ m}^2 \text{ g}^{-1}$ ) (Superfine 4; Alcan Chemicals, Alcan Aluminum Corp., Cleveland, Ohio) and a high surface area gibbsite ( $16.8 \text{ m}^2 \text{ g}^{-1}$ ) (Space Rite; Alcoa, Aluminum Company of America, Pittsburgh, Pennsylvania). Both of these gibbsites were pre-

cipitated under highly alkaline conditions ( $\text{pH} \geq 14$ ). The low surface area (LSA) gibbsite was used in Co-only, NTA-only and CoNTA experiments, whereas the high surface area (HSA) gibbsite was used solely for Co-only experiments. In addition,  $\delta\text{-Al}_2\text{O}_3$  ( $100 \text{ m}^2 \text{ g}^{-1}$ ) (Degussa Corp., Tererboro, New Jersey) was used in the Co-only experiments. Prior to use, both the LSA and HSA gibbsites and the  $\delta\text{-Al}_2\text{O}_3$  were treated for 30 min with 0.01 M NaOH to minimize dissolution of a small but highly soluble portion of the solid during adsorption experiments. Following this treatment, the solid was centrifuged and rinsed with 0.01 M  $\text{NaClO}_4$  a minimum of 7 times until the pH of the supernatant was 8.2 or less; then the solid was stored wet at 4 °C until use. The measured  $\text{N}_2$  BET (Brunauer, Emmett and Teller) surface areas of the treated solids were in agreement with the manufacturer's specification. The  $\text{pH}_{\text{pzc}}$  of the treated LSA gibbsite was determined by potentiometric titration and found to be 11 (McKinley et al. 1995). The  $\text{pH}_{\text{pzc}}$  of HSA gibbsite was not measured; however, based upon literature values for gibbsite (Hingston et al. 1972; Kavanagh et al. 1975; Hiemstra et al. 1987), the  $\text{pH}_{\text{pzc}}$  for the HSA gibbsite is expected to be  $10 \pm 1$ . The  $\text{pH}_{\text{pzc}}$  of the  $\delta\text{-Al}_2\text{O}_3$  was 9.2 (Girvin et al. 1993). X-ray diffraction (XRD) analysis of the LSA and HSA gibbsites using  $\text{CuK}\alpha$  radiation showed typical crystallographic spacings for gibbsite, with diffraction maxima at 4.85, 4.37, 3.35, 3.18, 2.45 and 2.38 Å. There were no discernable differences between the diffraction characteristics of the 2 gibbsites.

Based on the ideal structure of gibbsite (Davis and Hem 1989; Hsu 1989), the gibbsites used in this study have 2 types of surface hydroxyls on the hydrated crystals' faces. The oxygen of the  $\text{OH}^-$  groups on the basal plane surface is coordinated to 2 structural Al ions. This is referred to as a doubly coordinated surface hydroxyl. At the edge faces of gibbsite, the surface groups consist of 1  $\text{OH}^-$  and 1  $\text{H}_2\text{O}$  coordinated to a single structural Al. These singly coordinated aluminum edge sites,  $\equiv\text{Al}(\text{OH})(\text{H}_2\text{O})$ , act as Lewis acids, and are considered to be much more reactive than the basal plane doubly coordinated OH groups (Parfitt et al. 1977; Davis and Hem 1989; Hsu 1989). We will refer to  $\equiv\text{Al}(\text{OH})(\text{H}_2\text{O})$  as the reactive sites on gibbsite in the results and discussion that follow.

The properties of the sorbents used here are summarized in Table 1 and compared to those of an extensively investigated gibbsite prepared under acid conditions (pH 4.6) using the method of Gastuche and Herbillion (1962). In the remainder of this paper, the LSA gibbsite will be referred to as "gibbsite" because most of the data presented are for the LSA gibbsite. When comparing the Co-only adsorption by the 2 gibbsites, the LSA and HSA designations will be used.

Table 1. Properties of selected Al oxides.

Mineral (source)	Total BET surface area (m <sup>2</sup> g <sup>-1</sup> )	Edge face surface area (estimated) (m <sup>2</sup> g <sup>-1</sup> )	Site density (sites/nm <sup>2</sup> )	Nominal particle diameter <sup>¶¶¶</sup> (μm)	PZC
LSA Gibbsite† (Alcan)	3.4¶	nd‡‡	nd	1.3	11†††
HSA Gibbsite† (Alcoa)	16.8¶	nd	nd	0.25	nd
δ-Al <sub>2</sub> O <sub>3</sub> ‡ (Degussa)	101¶	na§§	1.3¶¶ (total) 8.5## (total)	0.013	9.2‡‡‡
Gibbsite§	19.8#	3.4#	9.6# (edge)		
	45††	9††	4†† (edge)	0.57###	9–10§§§

† Prepared at pH ≥ 14 and used in this study.

‡ Aluminum oxide C produced in oxyhydrogen flame and used in this study.

§ Prepared at pH 4.6 using method of Gastuche and Herbillon (1962). Not used in this study or commercially available.

¶ Measured after treatment with 0.01 M NaOH.

# Hiemstra et al. 1987.

†† Parfitt et al. 1977.

‡‡ Not determined.

§§ Not applicable.

¶¶ Back titration (Kummert and Stumm 1980).

## Tritium exchange (Kummert and Stumm 1980).

††† Potentiometric titration at 0.001, 0.01 and 0.1 M NaClO<sub>4</sub> (McKinley et al. 1995).

‡‡‡ Electrophoretic mobility in 0.01 M NaClO<sub>4</sub> (Girvin et al. 1993).

§§§ Potentiometric titrations at several ionic strengths (Hingston et al. 1972; Kavanagh et al. 1975; Hiemstra et al. 1987).

¶¶¶ Manufacturer's specification.

### Estimated distance between opposing corners of hexagonal crystals (Hiemstra et al. 1987).

## Adsorbates

The <sup>60</sup>Co (specific activity = 570 mCi/mg, 99% pure, Dupont, New England Nuclear, Billerica, Massachusetts) was added to <sup>59</sup>Co in the pH 2 working stock at 1:7300. The <sup>14</sup>C-NTA (specific activity = 11.5 mCi/mmol, 99.9% pure, ICN Biochemicals, Irvine, California) was added to unlabeled NTA in working stock at 1 to 1.57. The Co-NTA stock was prepared by mixing equal-molar quantities of Co and NTA from stock solutions described above and adjusting the pH to 7.

## Experimental Procedure and Analysis

Batch adsorption experiments were conducted for total NTA or Co-NTA concentrations of 1 μM, in 7.5 g L<sup>-1</sup> suspensions of gibbsite, at 25 ± 1 °C, with background electrolyte concentrations ranging from 0.01 to 1 M NaClO<sub>4</sub>. In addition, experiments were conducted with 0.5 μM CoNTA in 75 g L<sup>-1</sup> gibbsite suspensions and with 10 μM CoNTA in 0.5 g L<sup>-1</sup> gibbsite suspensions at 0.01 M NaClO<sub>4</sub>. Experiments were performed under an N<sub>2</sub> atmosphere to minimize dissolved CO<sub>2</sub> in solution and thus the possibility of CoCO<sub>3</sub> precipitation at high pH. Adsorption was measured as a function of pH (5 < pH < 10) as described by Girvin et al. (1993). Apparent adsorption equilibrium was reached in less than 4 h; however, all experiments were conducted for 24 h. Adsorption of Co and NTA was quantified by dual-labeled scintillation counting of <sup>60</sup>Co and <sup>14</sup>C-labeled NTA remaining in solution after filtration (0.1 μm). An independent measure of Co ad-

sorption was obtained by γ-counting of the 1.17- and 1.33-Mev gamma rays accompanying the <sup>60</sup>Co beta decay. For all experiments, the 2 independent determinations of <sup>60</sup>Co activity agreed within 3%. Dissolved Al in suspensions was measured by inductively coupled plasma mass spectrometry (ICP-MS) after filtration with prewashed 1.8-nm (25,000-MW) Amicon filters (Amicon, Danvers, Massachusetts). Total inorganic carbon was measured in filtered (0.1-μm) samples using a Dohrmann DC-80 carbon analyzer (Rosemount Analytical, Santa Clara, California). Aqueous speciation and solubility calculations for measured Co, NTA and dissolved Al concentrations were performed using MINTEQA (Felmy et al. 1984). These calculations were based on the stability constants and solubility products listed in Table 2 and excluded possible surface complexation (adsorption) reactions. Modeling of Co adsorption by gibbsite was performed with FITEQL (Westall 1982a, 1982b), using the Triple-Layer Model (TLM) (Davis and Leckie 1978; Sposito 1984; Hayes and Leckie 1987) and the TLM parameters for the LSA gibbsite (Table 3; McKinley et al. 1995).

## RESULTS AND DISCUSSION

### Dissolved Inorganic Carbon and Aluminum

Inorganic carbon was present in experimental suspensions, even though experiments were conducted under an N<sub>2</sub> atmosphere. However, the concentration of CoCO<sub>3</sub> (aq) was 10<sup>5</sup>-fold less than dominant Co species over the range of pH examined. Solutions were

Table 2. Thermodynamic stability constants:  $T = 25\text{ }^\circ\text{C}$ ,  $I = 0$  (Martell and Smith 1974, unless otherwise noted).

Chelate acidity:		
$\text{H}^+ + \text{NTA}^{3-} = \text{HNNTA}^{2-}$		10.29
$\text{H}^+ + \text{HNNTA}^{2-} = \text{H}_2\text{NTA}^{-}$		2.91
$\text{H}^+ + \text{H}_2\text{NTA}^{-} = \text{H}_3\text{NTA}$		2.01
Metal hydrolysis:†		
$\text{H}_2\text{O} = \text{H}^+ + \text{OH}^-$		-14.0
$\text{Co}^{2+} + \text{H}_2\text{O} = \text{CoOH}^+ + \text{H}^+$		-9.67
$\text{Co}^{2+} + 2\text{H}_2\text{O} = \text{Co}(\text{OH})_2 + 2\text{H}^+$		-18.77
$\text{Al}^{3+} + \text{H}_2\text{O} = \text{AlOH}_2^+ + \text{H}^+$		-4.99
$\text{Al}^{3+} + 2\text{H}_2\text{O} = \text{Al}(\text{OH})_2^+ + 2\text{H}^+$		-10.1
$\text{Al}^{3+} + 3\text{H}_2\text{O} = \text{Al}(\text{OH})_3 + 3\text{H}^+$		-16.0
$\text{Al}^{3+} + 4\text{H}_2\text{O} = \text{Al}(\text{OH})_4^- + 4\text{H}^+$		-23.0
Metal complexation:		
$\text{Na}^+ + \text{NTA}^{3-} = \text{NaNTA}^{2-}$		1.86
$\text{Co}^{2+} + \text{NTA}^{3-} = \text{CoNTA}^-$		11.66
$\text{Co}^{2+} + 2\text{NTA}^{3-} = \text{Co}(\text{NTA})_2^{4-}$		4.97
$\text{Co}^{2+} + \text{NTA}^{3-} + \text{H}_2\text{O} = \text{CoOHNTA}^{2-} + \text{H}^+$		0.44
$\text{Al}^{3+} + \text{NTA}^{3-} = \text{AlNTA}$		13.68
$\text{Al}^{3+} + \text{NTA}^{3-} + \text{H}^+ = \text{AlHNTA}^+$		15.58
$\text{Al}^{3+} + \text{NTA}^{3-} + \text{H}_2\text{O} = \text{AlOHNTA}^- + \text{H}^+$		8.34
$\text{Al}^{3+} + \text{NTA}^{3-} + 2\text{H}_2\text{O} = \text{Al}(\text{OH})_2\text{NTA}^{2-} + 2\text{H}^+$		0.45
Solubility products		
$\text{Al}(\text{OH})_3(\text{am})$	$\text{Al}^{3+} + 3\text{H}_2\text{O} = \text{Al}(\text{OH})_3(\text{am}) + 3\text{H}^+$	-10.38
$\text{Al}(\text{OH})_3(\text{c})$ (gibbsite)	$\text{Al}^{3+} + 3\text{H}_2\text{O} = \text{Al}(\text{OH})_3(\text{c}) + 3\text{H}^+$	-8.77
$\text{Co}(\text{II})\text{CO}_3(\text{s})$ (sphaerocobaltite)	$\text{Co}^{2+} + \text{CO}_3^{2-} = \text{Co}(\text{II})\text{CO}_3(\text{s})$	10.14‡
$\text{Co}(\text{II})(\text{OH})_2(\text{s})$ (transvaalite)	$\text{Co}^{2+} + 2\text{H}_2\text{O} = \text{Co}(\text{II})(\text{OH})_2(\text{s}) + 2\text{H}^+$	-12.08‡

† Ball et al. (1980).

‡ Naumov et al. (1974).

undersaturated with respect to  $\text{CoCO}_3(\text{s})$  and  $\text{Co}(\text{OH})_2(\text{s})$  (Table 2).

The interpretation of NTA and CoNTA adsorption and the calculation of their aqueous speciation required the measurement of dissolved Al, because: 1) NTA enhances the solubility of Al oxides (Elliott and Huang 1979); and 2) dissolved Al will compete with Co for NTA, as evidenced by comparison of Al and Co stability constants for NTA in Table 2. Figure 1 shows measured and calculated dissolved Al concentrations in the presence and absence of  $1\text{ }\mu\text{M}$  NTA. Calculated Al concentrations represent  $\text{Al}(\text{OH})_3(\text{am})$  and gibbsite solubility. All aqueous speciation calculations used measured Al concentrations in  $1\text{ }\mu\text{M}$  NTA gibbsite suspensions. Measured Al was in good agreement with the calculated solubility of gibbsite

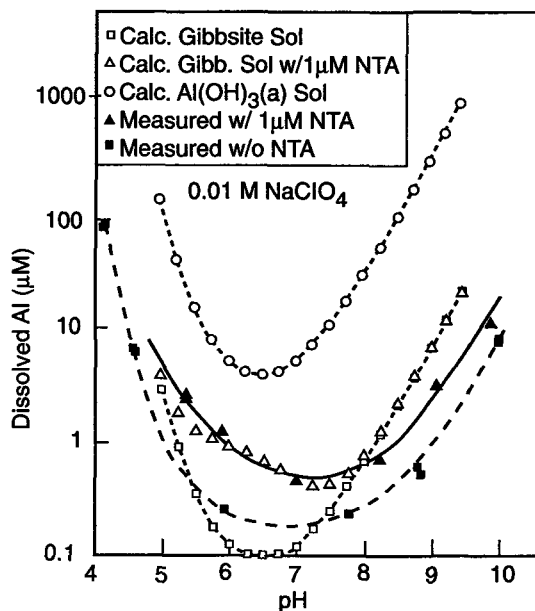


Figure 1. Dissolved Al concentration measured in gibbsite suspensions (solid points) and calculated (with MINTeq code) concentrations (open points) in equilibrium with amorphous  $\text{Al}(\text{OH})_3$  and with gibbsite in the absence of NTA and gibbsite in the presence of  $1\text{ }\mu\text{M}$  NTA. Solid and dashed curves through measured values are non-linear least-squares fits to measured values.

in the presence of  $1\text{ }\mu\text{M}$  NTA, although for  $\text{pH} > 8$  the experimental curve fell below the calculated solubility. A similar difference in the absence of NTA was apparent.

#### Adsorption at Low Ionic-Strength ( $0.01\text{ M NaClO}_4$ )

The adsorption of Co-only was cation-like and NTA-only ligand-like (Figure 2a). Adsorption of Co in the presence of equal-molar NTA (referred to as Co with NTA) was essentially cation-like, with some suppression of adsorption for  $\text{pH} > 7.6$  relative to Co-only adsorption (Figure 2a). Below  $\text{pH} = 6.7$ ,  $\text{Co}^{2+}$  was the dominant Co species (Figure 2c), because Al displaced Co from the NTA. Thus, for  $\text{pH} < 6.7$ , cation-like Co adsorption would be expected and was observed. Aqueous speciation calculations suggest that, for  $\text{pH} > 6.7$ ,  $\text{CoNTA}^-$  was a major species. This would suggest ligand-like adsorption of Co with NTA for  $\text{pH} > 6.7$ , but this was not observed. All aqueous speciation calculations presented here ignore the competitive effects of adsorption on the multiple aqueous equilibria.

Table 3. Triple-layer model parameters for low surface area gibbsite (McKinley et al. 1995).

Surface area = $3.4\text{ m}^2\text{ g}^{-1}$		Site density = 6 sites/ $\text{nm}^2$	
Capacitance ( $\text{F}/\text{m}^2$ ):		$C_1 = 1.2$ ; $C_2 = 0.2$	
Acidity constants:		$\log K_{a1} = 12.30$ ; $\log K_{a2} = -13.16$	
Complexation constants:		$\log K_{\text{Na}} = -10.37$ ; $\log K_{\text{ClO}_4} = 10.15$	

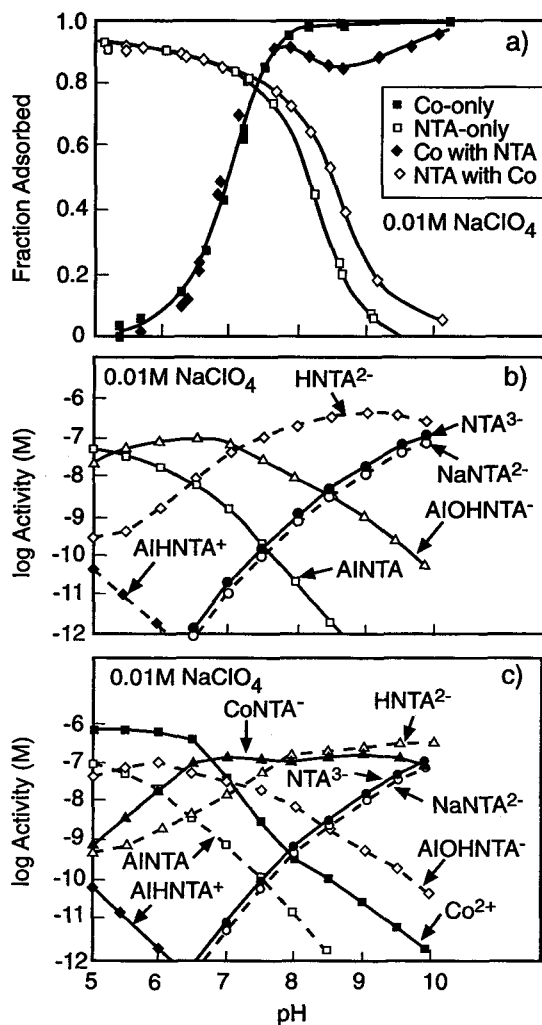


Figure 2. Adsorption and aqueous speciation in suspensions containing  $1 \mu\text{M}$  total Co, NTA or Co-NTA (equal molar),  $7.5 \text{ g L}^{-1}$  gibbsite and  $0.01 \text{ M NaClO}_4$ . (a) Adsorption edges for Co-only, NTA-only and equal molar Co-NTA. (b) Calculated NTA aqueous speciation using measured NTA and Al solution concentrations. (c) Calculated Co-NTA aqueous speciation using measured Co, NTA and Al solution concentrations.

The similarity of the Co with NTA adsorption edge to that of the Co-only adsorption edge for  $\text{pH} > 6.7$  (Figure 2a) suggests that the aluminol sites were out-competing NTA for Co. That is, the formation of a Co surface complex was thermodynamically favored over that of the aqueous  $\text{CoNTA}^-$  complex. This was consistent with the modest strength of the equilibrium constant for the aqueous  $\text{CoNTA}^-$  complex ( $\log K = 12$ ) relative to that of  $\text{CoEDTA}^{2-}$  ( $\log K = 17$ ), for which ligand-like adsorption of Co with EDTA was observed for  $5 < \text{pH} < 10$  on  $\delta\text{-Al}_2\text{O}_3$  (Girvin et al. 1993). However, for  $\text{pH} > 7.6$  the suppression of the Co with NTA edge with respect to the Co-only edge

and the increase in NTA adsorption in the presence of Co (referred to as NTA with Co) with respect to the NTA-only edge (Figure 2a) suggested the formation of a ternary CoNTA surface complex in this pH region. This was reasonable based on the structure of the tetradentate CoNTA complex (Rabenstein and Kula 1969) (Figure 3a). Coordination of the central Co with the nitrogen and 3 carboxylate oxygens leaves 2 waters of hydration remaining. One of these waters is in the equatorial plane formed by coordination of the nitrogen and 2 oxygens with the Co, and the other water is axial to the Co and the third carboxylate oxygen. Following the notation of Schindler (1990), a Type A ternary CoNTA surface complex may be formed when one or two of the remaining waters of hydration in CoNTA coordinate with an  $\equiv\text{Al}(\text{OH})(\text{H}_2\text{O})$  edge site(s) forming either an inner- or outer-sphere surface complex (Figure 3b). Electron spin resonance spectroscopy of wet gibbsite films having been contacted with Cu-glycine at various pH values suggests that Type A ternary surface  $\text{Cu}(\text{gly})^-$  and  $\text{Cu}(\text{gly})_2$  complexes occur (McBride 1985). Although steric constraints may differ, the observations of McBride (1985) support the existence of a ternary surface complex in our Co-NTA-gibbsite system because of the similarity in the coordinating ligands in Cu-glycine and Co-NTA.

Evidence for the formation of a ternary  $\text{CoNTA}^-$  surface complex was observed over a wide range of sorbate to sorbent ratios (total  $\text{CoNTA}^-$  to gibbsite =  $0.5 \mu\text{M}:75 \text{ g L}^{-1}$  and  $10 \mu\text{M}:0.5 \text{ g L}^{-1}$ ). Adsorption edges under these conditions (data not shown) were similar to edges shown in Figure 2a, with the NTA with Co edge greater than the NTA-only edge for  $\text{pH} > 7.5$  and the Co with NTA edge suppressed relative to the Co-only edge for  $\text{pH} > 7.5$ . Thus, the formation of a ternary  $\text{CoNTA}^-$  surface complex appears to occur over the range of sorbate:sorbent ratios. Below  $\text{pH} 7.5$ , NTA with Co adsorption was identical to NTA-only adsorption (Figure 2a). For the Co-NTA system, the aqueous speciation of NTA for  $\text{pH} < 7$  was identical to that of the NTA-only system (compare Figures 2b and 2c), suggesting that  $\text{AIOHNTA}^-$ ,  $\text{AINTA}$  or  $\text{AIHNTA}^+$  is the possible adsorbed NTA species. The nature of the adsorbed Co, NTA and CoNTA species is discussed below.

#### Adsorption at High Ionic Strength ( $1 \text{ M NaClO}_4$ )

**NTA-ONLY ADSORPTION.** For  $\text{pH} > 8.5$ , the  $1 \text{ M NaClO}_4$  edge no longer parallels the  $0.01 \text{ M NaClO}_4$  edge, but rather levels off between 0.1 and 0.2 fractional adsorption units (Figure 4a). This difference was attributed to adsorption of  $\text{NaNTA}^{2-}$  in the  $1 \text{ M NaClO}_4$  system, where the dominant aqueous species was  $\text{NaNTA}^{2-}$  for  $\text{pH} > 8.5$  (Figure 4b). In the  $0.01 \text{ M NaClO}_4$  system,  $\text{NaNTA}^{2-}$  was only a minor species in this pH range (Figure 2b). The adsorption of

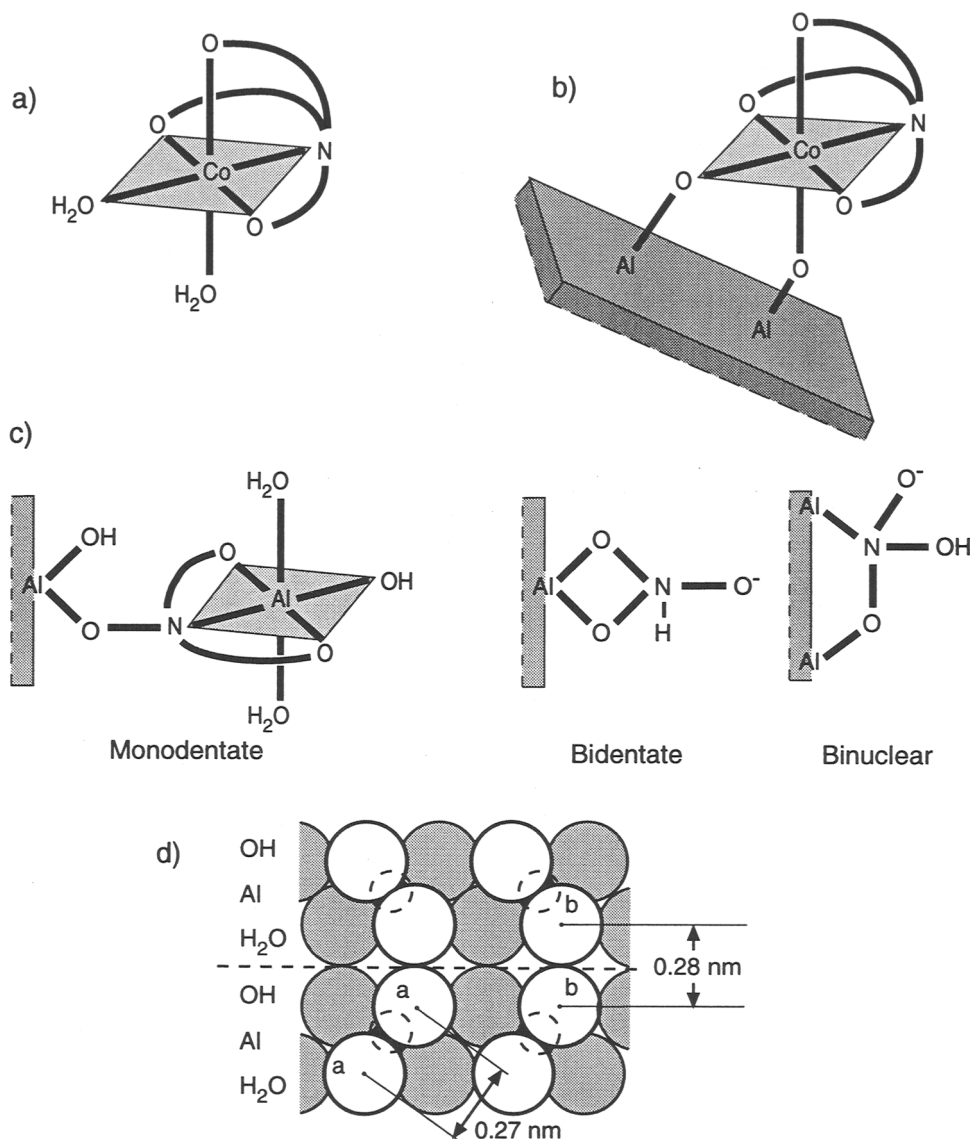
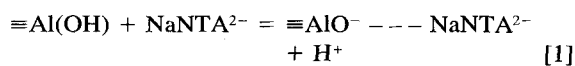


Figure 3. (a) Structure of 1:1 Co-NTA solution complex. (b) Proposed coordination of outer-sphere ternary CoNTA<sup>-</sup> surface complex on gibbsite edge faces. (c) Proposed monodentate, bidentate and binuclear surface complexes for NTA-only adsorption on gibbsite edge faces. (d) Arrangement of edge sites on the idealized 100 or 110 edge faces of gibbsite. Spacing between the OH-H<sub>2</sub>O pair of a single Al(OH)(H<sub>2</sub>O) edge site (labeled "a") and between the OH and H<sub>2</sub>O of adjacent edge sites (labeled "b") (Parfitt et al. 1977; Bragg and Claringbull 1965). Dashed line represents hydrogen bonded interface between successive layers of Al atoms.

NaNTA<sup>2-</sup> should be relatively weak (electrostatically bound), because NaNTA<sup>2-</sup> adsorbs only when it becomes the dominant solution species. The formation of an outer-sphere NaNTA<sup>2-</sup> surface complex is proposed by the equation:



where we have dropped the H<sub>2</sub>O in the designation of the aluminol site for clarity and used the notation "---" to indicate that NaNTA<sup>2-</sup> is outer-sphere.

For pH < 8.5, the shift of the NTA-only edge at 1 M NaClO<sub>4</sub> relative to the NTA-only edge at 0.01 M NaClO<sub>4</sub> was small. The pH at which 50% adsorption occurs ( $\Delta\text{pH}_{50}$ ) decreased by 0.2 pH units from 8.15 to 7.95 (Figure 4a). The  $\Delta\text{pH}_{50}$  values for edges at 0.1 and 0.5 M NaClO<sub>4</sub> (data not shown) were successively displaced to lower pH values relative to that of the 0.01 M edge and fell between the  $\Delta\text{pH}_{50}$  values of the 0.01 and 1 M edges. The magnitude of shifts in anion- and cation-like adsorption edges with ionic strength have been used to evaluate the importance of electro-

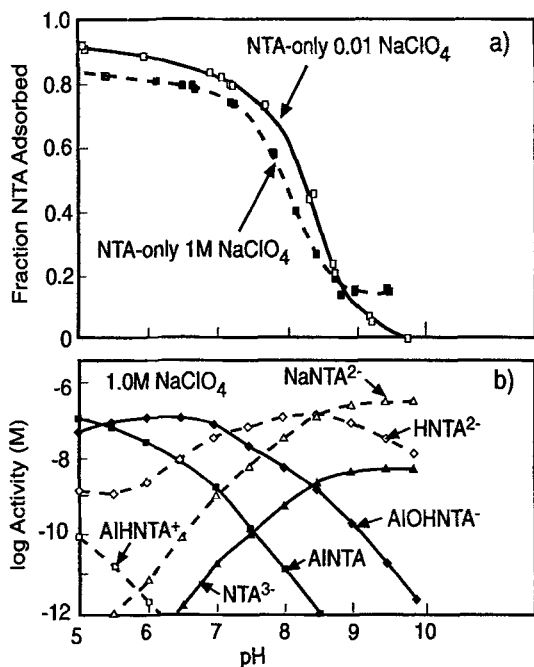
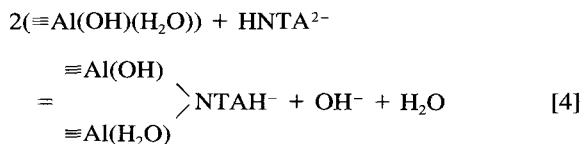
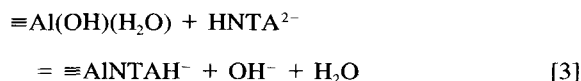
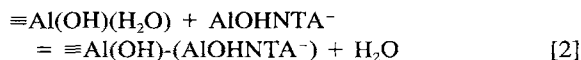


Figure 4. Adsorption and aqueous speciation in suspensions containing  $1 \mu\text{M}$  total NTA and  $7.5 \text{ g L}^{-1}$  gibbsite. (a) Shift in NTA-only adsorption edge with ionic strength. (b) Calculated NTA aqueous speciation at  $1 \text{ M NaClO}_4$  using measured NTA and Al solution concentrations.

static contributions to the free energy of adsorption (Hayes et al. 1987). Minimal displacement of edges with changes in ionic strength indicated that electrostatic interactions were of secondary importance relative to specific chemical bonding of sorbate moieties to sorbent surface functional groups or structural metal ions of hydrous oxides. The  $\Delta\text{pH}_{50} = 0.2$  observed here for NTA was similar to that observed (Hayes 1987; Hayes et al. 1987) for inner-sphere complexation of selenite by goethite, for the same change in ionic strength. This  $\Delta\text{pH}_{50}$  shift indicated that the NTA surface complexes were relatively insensitive to electrostatic effects associated with changes in ionic strength. By analogy with the observations of Hayes, NTA may form inner-sphere surface complexes with the aluminol edge sites of gibbsite ( $\equiv\text{Al}(\text{OH})(\text{H}_2\text{O})$ ). The formation of a strong inner-sphere NTA (or HNTA) complex was consistent with the observation that free HNTA is more strongly adsorbed than the CuNTA chelate by  $\delta\text{-Al}_2\text{O}_3$  for  $4 < \text{pH} < 6.5$  (Elliott and Huang 1979).

Assuming that surface Al-NTA complexes are analogous to those formed in solution (Figures 2b and 4b) and invoking the inner-sphere hypothesis, we propose the following monodentate, bidentate, and binuclear ligand exchange reactions describing NTA adsorption:



The placement of NTA immediately to the right of the  $\equiv\text{Al}$  in Equation 3 and the “-” in Equations 2 and 4 are used to indicate the formation of inner-sphere NTA complexes. The monodentate coordination (Equation 2) of the intact AIOHNTA<sup>-</sup> complex is via one carboxylate oxygen which has unwrapped from the central Al ion (Figure 3c). The carboxylate bonds to the central metal ions of aqueous NTA chelates are quite labile (Rabenstein and Kula 1969), and the unwrapped carboxylate oxygen could coordinate to the edge site Al by displacing a water. The bidentate surface complex (Equation 3) represents coordination of 2 NTA carboxylate oxygens to a single aluminol group (Figure 3c). The binuclear NTA complex (Equation 4) represents coordination of 2 carboxylate oxygens with adjacent aluminol sites and/or coordination of the nitrogen and a carboxylate oxygen to adjacent aluminol groups (Figure 3c).

The similarity in the distance between the N and the carboxylate oxygen atoms of NTA and the spacing between gibbsite's edge site aluminol oxygens is consistent with the formation of bidentate (Equation 3) and binuclear (Equation 4) NTA surface complexes. The N-to-carboxylate-O distance in the fully extended glycinate arm of NTA is 0.28 nm. This was based on the bond angles and lengths for glycine (CRC 1977). The distances between carboxylate oxygens of NTA can vary over a wide range (0.27–0.55 nm). On the 100 and 110 edge faces of gibbsite, the O-O distance between the OH-H<sub>2</sub>O pair in a “single”  $\equiv\text{Al}(\text{OH})(\text{H}_2\text{O})$  edge site is 0.27 nm (Bragg and Claringbull 1965), while the O-O distance separating the OH and H<sub>2</sub>O coordinated to “adjacent” edge sites, located in successive hydrogen bonded layers, is 0.28 to 0.29 nm (Saalfeld 1960; Bragg and Claringbull 1965) (Figure 3d). The similarity in these distances suggests that a bidentate NTA surface complex (Equation 3) could form via exchange of an OH-H<sub>2</sub>O pair (labeled “a”, Figure 3d) with 2 NTA carboxylate oxygens. For the binuclear NTA surface complex (Equation 4), the N and carboxylate O or the 2 carboxylate oxygens of the NTA exchange with the OH and H<sub>2</sub>O (labeled “b”, Figure 3d) from adjacent edge sites. The proposed bidentate and binuclear NTA surface complexes are also supported by studies of oxalate and phosphate sorption by gibbsite. The adsorption of oxalate (Parfitt et al.

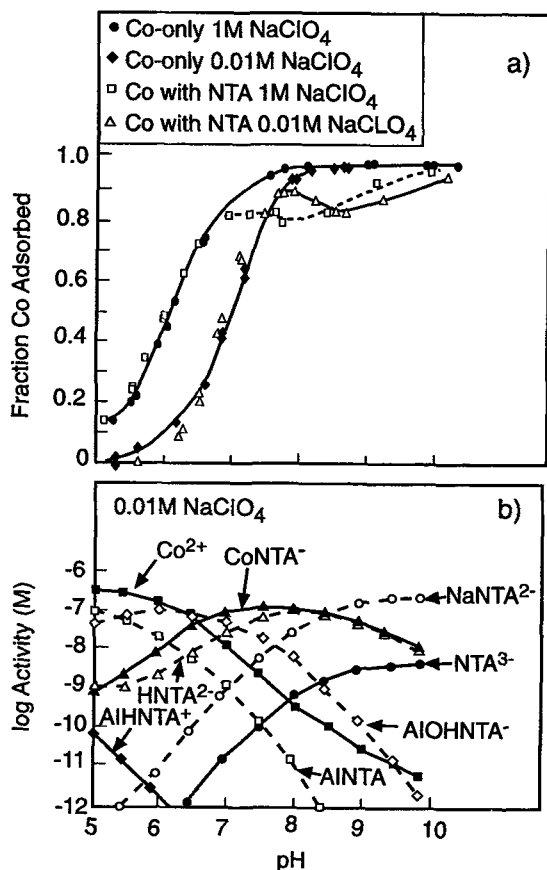


Figure 5. (a) Shift in Co adsorption edges with ionic strength for suspensions containing  $1 \mu\text{M}$  total Co-only or Co-NTA (equal molar) and  $7.5 \text{ g L}^{-1}$  gibbsite. (b) Calculated aqueous speciation for  $1 \mu\text{M}$  total Co-NTA (equal molar) at  $1 \text{ M NaClO}_4$  using measured Co, NTA and Al solution concentrations.

1977) and phosphate (Kyle et al. 1975) by gibbsite were described by both bidentate coordination to a single edge site and binuclear coordination between adjacent edge sites. The O-O distance for oxalate was given as  $0.28 \text{ nm}$  and for phosphate,  $0.29 \text{ nm}$  (Parfitt et al. 1977; Kyle et al. 1975). Infrared spectra of oxalate adsorbed to gibbsite was consistent with the bidentate and binuclear coordination (Parfitt et al. 1977).

A significant fraction of the phosphate sorbed to gibbsite was only slowly desorbed (Hingston et al. 1974). This fraction increased with decreasing pH. The isotopic exchange of phosphate adsorbed onto gibbsite was also very slow, and was classified as inert in the pH range 5 to 6, where the exchange half-life was 50 to 4 h, respectively (Kyle et al. 1975). The slow desorption and isotopic exchange of phosphate was attributed to the bidentate and binuclear bonding of phosphate on gibbsite edge faces (Hingston et al. 1974; Kyle et al. 1975).

The similarity in the O-O distances of oxalate and phosphate with the N-O distance of NTA suggests that NTA bonding to gibbsite should be predominantly bidentate and/or binuclear. If this is correct, then the desorption of NTA from gibbsite will be slow, and will decrease as pH decreases, as was found for phosphate. This was precisely what we observed in a separate study (Bolton and Girvin 1996) where we examined NTA and equal molar Co-NTA desorption from LSA gibbsite using a stir-flow cell (Seyfried et al. 1989; Bar-Tal et al. 1990). Experiments were conducted in both the continuous flow and stop-flow modes, and desorption rates were measured at several fixed pH values and influent flow rates for conditions similar to those used here. Desorption of  $1 \mu\text{M}$  NTA into  $0.01 \text{ M NaClO}_4$  was strongly pH dependent with desorption half-lives of 1 h at pH 8 and 80 h at pH 6. For equal molar Co-NTA adsorbed to gibbsite at pH 7 ( $1 \mu\text{M}$  total Co-NTA), Co and NTA desorption ( $0.01 \text{ M NaClO}_4$ ) were independent of one another, with desorption half-lives of 2 and 17 h, respectively. This independent desorption of Co and NTA is consistent with the independence of cation-like and anion-like adsorption edges for equal molar Co-NTA (Figure 2a). The slow desorption of NTA at pH 7 and 6 is consistent with the formation of bidentate and binuclear NTA complexes with decreasing pH. Nuclear magnetic resonance studies of solution NTA show that the N-protonated HNTA<sup>2-</sup> isomer dominates for  $7 < \text{pH} < 10$ , whereas for  $\text{pH} < 5$  the carboxylate-protonated isomer begins to dominate (Rabenstein and Kula 1969). This shift in the proton increases the reactivity of the N with decreasing pH and thus may enhance binuclear coordination of the nitrogen and carboxylate oxygen to adjacent edge sites. This may account for the increase in the NTA desorption half-lives with decreasing pH. Although there is no direct evidence for the formation of bidentate and binuclear NTA surface complexes, the information presented here is consistent with their formation.

ADSORPTION OF CO-ONLY AND CO IN THE PRESENCE OF NTA. The adsorption edges for Co-only and Co in the presence of equal molar NTA (Co with NTA) showed similar behavior in both  $1 \text{ M}$  and  $0.01 \text{ M NaClO}_4$  suspensions (Figure 5a). Both the Co-only and Co with NTA edges are displaced to lower pH at the higher ionic strength ( $\Delta\text{pH}_{50} = -1$ ). This enhanced adsorption of Co by gibbsite with increasing ionic strength has not been reported previously for other Al, Fe or Si oxides.

Cobalt-only edges were also measured for 0.01 and  $1 \text{ M NaClO}_4$  suspensions of high surface area (HSA) gibbsite ( $33 \text{ m}^2 \text{ L}^{-1}$ ) and Degussa  $\delta\text{-Al}_2\text{O}_3$  ( $50 \text{ m}^2 \text{ L}^{-1}$ ) and compared to the LSA gibbsite ( $26 \text{ m}^2 \text{ L}^{-1}$ ) edges presented above. The high ionic strength enhancement in the Co-only adsorption observed for the LSA gibbs-



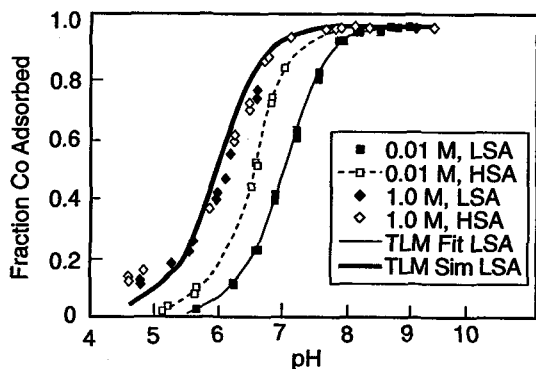
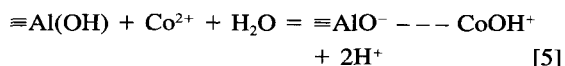


Figure 6. Shift in Co-only adsorption edges with ionic strength for  $7.5 \text{ g L}^{-1}$  low surface area (LSA) gibbsite and  $2 \text{ g L}^{-1}$  high surface area (HSA) gibbsite ( $1 \mu\text{M}$  total Co,  $\text{NaClO}_4$  electrolyte). Solid line is triple-layer model "fit" to  $0.01 \text{ M}$  edge with outer-sphere  $\equiv\text{AlO}^-$  ---  $\text{CoOH}^+$  surface ion-pair and the bold line is a simulation of  $1 \text{ M}$  edge with the log  $K$  from the  $0.01 \text{ M}$  "fit."

ite (Figure 5a) was also observed for the HSA gibbsite, with  $\Delta\text{pH}_{50} = -0.5$  between the  $0.01$  and  $1.0 \text{ M}$   $\text{NaClO}_4$  edges of HSA gibbsite (Figure 6). However, no ionic strength shift was observed with  $\delta\text{-Al}_2\text{O}_3$  (data not shown).

All 3 of the Al oxides investigated were treated with strong base prior to use. The Co-only experiments were repeated at  $0.01$  and  $1.0 \text{ M}$   $\text{NaClO}_4$  for all 3 oxides using untreated solids to determine if ionic strength shifts in Co edges on LSA and HSA gibbsite were an artifact of the base treatment. In all cases, the Co-only edges of the untreated oxides (data not shown) were identical to those of the treated oxides. The formation of inner-sphere Co surface complexes with  $\delta\text{-Al}_2\text{O}_3$  (Brown 1990; Chisholm-Brause et al. 1990, 1991) would account for the lack of any ionic strength shift in our Co edges on  $\delta\text{-Al}_2\text{O}_3$ . Similarly, Hayes and Leckie (1987) observed little or no shift in Pb and Cd adsorption edges between goethite suspensions at  $0.01$  and  $1.0 \text{ M}$   $\text{NaNO}_3$  and successfully described adsorption at all ionic strengths using the triple-layer model (TLM) and inner-sphere Pb and Cd surface complexes. Extended X-ray adsorption fine structure (EXAFS) and pressure-jump kinetic studies confirmed the formation of inner-sphere complexes (Hayes 1987).

The enhanced adsorption of Co with increasing ionic strength reported here appears to be unique to gibbsite and precludes the formation of inner-sphere Co complexes on gibbsite. We have simulated the observed ionic strength shifts for Co-only adsorption on LSA gibbsite (Figures 5 and 6) using the TLM and a single outer-sphere surface complex described by:



The log  $K$  ( $=-11.69$ ) for this reaction was derived by optimizing the fit to the  $0.01 \text{ M}$  Co-only edge (Figure 6, solid line) using FITEQL and the TLM parameters for LSA gibbsite (Table 3). This log  $K$  was used to simulate the  $1 \text{ M}$  Co-only edge (Figure 6, solid line). The agreement between the simulated and observed  $1 \text{ M}$  Co-only edge was excellent, both having  $\Delta\text{pH}_{50} = -1$ . The outer-sphere surface complex  $\equiv\text{AlO}^-$  ---  $\text{Co}$  did not provide a good fit to the  $0.01 \text{ M}$  Co-only LSA edge and was not considered further due to the good fit provided by Equation 5 alone. As a check, reactions for inner-sphere surface complexes  $\equiv\text{AlOCo}$  and  $\equiv\text{AlOCoOH}$  were used to fit the  $0.01 \text{ M}$  Co-only edge. However, as expected, simulations at  $1 \text{ M}$   $\text{NaClO}_4$  using these log  $K$ s predicted no edge shift relative to the  $0.01 \text{ M}$  edge, in disagreement with observations.

The FITEQL simulations of  $1 \text{ M}$  edges were similar to the approach used by Hayes (1987). The Davies equation was not used to correct solution equilibrium constants; that is, the solution activity component in FITEQL, used at  $0.01 \text{ M}$ , was removed from the formulation. Activity coefficient corrections to relevant solution equilibrium constants and hydrogen ion concentration were made for  $1.0 \text{ M}$   $\text{NaClO}_4$ . These adjusted values were used for FITEQL simulations of  $1 \text{ M}$  edges. Because  $\text{Co}^{2+}$  was the dominant solution ion over the range of conditions considered, we have neglected activity corrections to Co hydrolysis products. The pH was converted to  $\text{H}^+$  concentration using the  $\text{H}^+$  activity coefficient,  $\gamma_{\text{H}} = 0.804$ . This  $\gamma_{\text{H}}$  was calculated using an independent chemical equilibrium model, GMIN (Felmy 1990), which incorporates Pitzer's activity coefficient formalism and interaction parameters valid at  $1 \text{ M}$ . This was the only correction made for the  $1 \text{ M}$  simulations. The TLM calculations described here using FITEQL were performed using the surface activity conventions of both Hayes and Leckie (1987) and Davis et al. (1978). The simulations at  $1 \text{ M}$  differed somewhat, in that the Hayes and Leckie convention predicted a  $-0.2 \text{ pH}$  unit greater  $\Delta\text{pH}_{50}$  shift than did the Davis convention. We have reported the latter because this convention was used by McKinley et al. (1995) to determine the TLM parameters (Table 3) for LSA gibbsite. The agreement between the simulated and observed edges at  $1 \text{ M}$  supports the hypothesis that Co forms outer-sphere complexes with LSA and HSA gibbsite.

We have suggested above that the suppression of the  $0.01 \text{ M}$  Co with NTA edge in the mid pH region, relative to the Co-only edge (Figures 2a and 5a), was due to the formation of a ternary surface complex. This feature in the  $1 \text{ M}$  Co with NTA edge (Figure 5a) further suggest this was the case for  $1 \text{ M}$   $\text{NaClO}_4$ . The pH at which this suppression started for the  $1 \text{ M}$   $\text{NaClO}_4$  Co with NTA edge was lowered by  $1 \text{ pH}$  unit relative to the  $0.01 \text{ M}$   $\text{NaClO}_4$  edge (Figure 5a). This

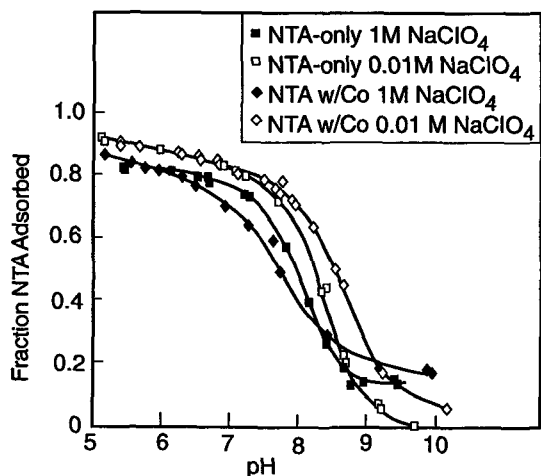
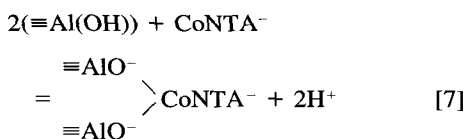


Figure 7. Shift in NTA with Co and NTA-only adsorption edges with ionic strength in suspensions containing  $1 \mu\text{M}$  total NTA or Co-NTA (equal molar) and  $7.5 \text{ g L}^{-1}$  gibbsite.

was consistent with the formation of a Type A ternary surface complex as opposed to a Type B ternary complex (Schindler 1990) in which the ligand coordinates with surface sites. The observed ionic strength shift in suppression of the Co with NTA edge and the success of outer-sphere modeling of the Co-only edges suggested that the association of the Co in the intact CoNTA complex with the surface is outer-sphere ion-pair formation. The following equations are proposed for mono- and bidentate Type A ternary surface complexes:



Equations 5 to 7 should describe the adsorption of Co in the Co-NTA-gibbsite system considered here. It is possible that a ternary CuNTA<sup>-</sup> surface complex, similar to our proposed CoNTA<sup>-</sup> ternary surface complex, was present in the Cu-NTA- $\delta$ -Al<sub>2</sub>O<sub>3</sub> system examined by Elliott and Huang (1979). Although not suggested by these authors, the presence of a CuNTA ternary surface complex is consistent with the adsorption behavior of Cu reported as a function of pH and the Cu to NTA concentration ratio. NTA adsorption in the NTA-only system should be completely described by Equations 1 through 4. In the Co-NTA system these same reactions plus Equations 6 and 7 should describe NTA adsorption.

NTA ADSORPTION IN THE PRESENCE OF CO. The adsorption of NTA in the presence of equal molar Co (NTA with

Co) at  $1.0 \text{ M NaClO}_4$  was substantially altered relative to that at  $0.01 \text{ M NaClO}_4$  (Figure 7) due to the presence of the ternary CoNTA<sup>-</sup> surface complex (Equations 6 and 7). Recall in the  $0.01 \text{ M NaClO}_4$  system that both the enhancement of NTA with Co adsorption relative to adsorption of NTA-only and the suppression of Co with NTA relative to Co-only adsorption for  $\text{pH} > 7.5$  (Figure 2a) was attributed to a ternary CoNTA<sup>-</sup> surface complex. The effect of an increase in ionic strength on the adsorption of the ternary CoNTA<sup>-</sup> complex can be seen by comparing Co with NTA and Co-only edges at  $0.01$  and  $1 \text{ M NaClO}_4$  (Figure 5). That is, the region where the ternary CoNTA<sup>-</sup> surface complex suppresses the Co with NTA edge relative to the Co-only edge was shifted to lower pH ( $\Delta\text{pH}_{50} = -1$ ) (Figure 5). We have suggested above that this was due to the outer-sphere nature of Equations 6 and 7. This ionic strength shift in the ternary CoNTA<sup>-</sup> complex manifested itself in the NTA with Co edge as a similar shift to lower pH, as seen by comparing the NTA with Co edges in Figure 7. Thus, this shift between the  $0.01$  and  $1.0 \text{ M NaClO}_4$  NTA with Co edges was not inconsistent with the minimum ionic strength shifts observed for the NTA-only system (Figures 4a and 7) and the proposed inner-sphere ligand exchange reactions (2 to 4) for NTA-only adsorption. The apparent difference in the NTA with Co and NTA-only edges at  $1 \text{ M NaClO}_4$  (Figure 7) was also due to the ionic strength shift in Co adsorption of the ternary CoNTA<sup>-</sup> complex. For  $\text{pH} > 8.3$ , the NTA with Co edge at  $1 \text{ M NaClO}_4$  leveled off and paralleled the pH axis (Figure 7) as did the NTA-only edge at  $1 \text{ M NaClO}_4$ . This behavior was attributed to adsorption of  $\text{NaNTA}^{2-}$  (Equation 1), because for  $\text{pH} > 8.5$  in the  $1 \text{ M NaClO}_4$  system the dominant aqueous species was  $\text{NaNTA}^{2-}$  (Figure 5b).

## SUMMARY AND CONCLUSIONS

The adsorption of Co by gibbsite in the presence of equal-molar NTA was predominantly cation-like for the range of conditions investigated here. Thus, the adsorption of Co in the presence of equal molar NTA would preclude NTA from significantly altering the mobility of <sup>60</sup>Co in soil pore waters and groundwaters where gibbsite is an important mineral sorbent. However, the cation-like adsorption of Co will be suppressed as the NTA:Co ratio increases. This is due to the more effective competition of NTA with the surface for Co as the NTA:Co ratio increases. Thus, at waste sites where  $\text{NTA}:\text{Co} \gg 1$  the NTA could alter the mobility of <sup>60</sup>Co in soil pore waters and groundwaters. However, enhanced <sup>60</sup>Co mobility may be short-lived due to the rapid bacterial degradation of NTA (Bolton et al. 1996; Bolton and Girvin 1996) via native microbial populations or specialized NTA degrading populations introduced as part of specific remediation strategies.

Cobalt adsorption by a low and high surface area gibbsite, both in the absence and in the presence of equal-molar NTA, strongly increased with increasing ionic strength from 0.01 to 1 M NaClO<sub>4</sub>. This enhanced adsorption of Co was unique to gibbsite and had not been previously reported. No change in Co adsorption for the same increase in ionic strength was observed for  $\delta$ -Al<sub>2</sub>O<sub>3</sub>, which is consistent with the formation of inner-sphere Co surface complexes on this solid. To describe the observed ionic strength dependence of Co adsorption on gibbsite, we have proposed that the outer-sphere ion-pairs,  $\equiv\text{AlO}^- \cdots \text{CoOH}^+$  and  $\equiv\text{AlO}^- \cdots \text{CoNTA}^-$ , form on the gibbsite surface. This was based on the ability of triple-layer model simulations to describe the observed ionic strength shifts in Co-only adsorption by LSA gibbsite. The enhanced adsorption of NTA at pH > 7.5 in the presence of Co, relative to that of NTA-only, is consistent with the formation of a Type A ternary surface complex.

We have proposed NTA adsorption on gibbsite to take place via the formation of inner-sphere monodentate, bidentate and binuclear surface complexes. The existence of bidentate and binuclear NTA surface complexes is consistent with the slow rates of NTA desorption reported elsewhere at pH 6 and 8 and at pH 7 in the presence of equal molar Co. Although we present no direct evidence of ternary CoNTA<sup>-</sup> and bidentate or binuclear NTA surface complexes, their existence on gibbsite edge faces is plausible based on data and arguments presented here. We are currently examining the ability of these and possibly other reactions to mechanistically describe the observed NTA adsorption behavior.

#### ACKNOWLEDGMENTS

This research was supported by the Subsurface Science Program, Office of Health and Environmental Research (OHER), US Department of Energy (DOE). The continued support of Dr. F. J. Wobber of OHER is greatly appreciated. Pacific Northwest National Laboratory is operated for DOE by Battelle Memorial Institute under Contract DE-AC06-76RLO 1830.

#### REFERENCES

- Ayers JA. 1970. Decontamination of nuclear reactors and equipment. New York: Ronald Pr. 164 p.
- Ball JW, Nordstrom DK, Jenne EA. 1980. Additional and revised thermodynamic data and computer code for WAT-EQ2—A computerized chemical model for trace and major element speciation and mineral equilibria of natural waters. Water Resources Investigations 78-116. Menlo Park, CA: US Geological Survey. 81 p.
- Bar-Tal A, Sparks DL, Pesek JD, Feigenbaum S. 1990. Analyses of adsorption kinetics using a stirred-flow chamber: I. Theory and critical tests. Soil Sci Soc Am J 54:1273-1278.
- Bolton H, Jr, Girvin DC. 1996. Effect of adsorption and aqueous speciation on the biodegradation of nitrilotriacetate by *chelatobacter heintzii*. Environ Sci Tech 30(3):931-938.
- Bourg CM, Schindler PW. 1979. Effect of ethylenediaminetetraacetic acid on the adsorption of copper(II) at amorphous silica. Inorg Nucl Chem Lett 15:225-229.
- Bowers AR. 1982. Adsorption characteristics of various metals at the oxide-solution interface: effect of complex formation [dissertation]. Newark, DE: Univ of Delaware. 202 p.
- Bowers AR, Huang CP. 1986. Adsorption characteristics of metal-EDTA complexes onto hydrous oxides. J Colloid Interface Sci 110:575-590.
- Bragg, WL, Claringbull GF. 1965. The crystalline state, vol 4. London: Bell and Sons. 118 p.
- Brown GE. 1990. Spectroscopic studies of chemisorption reaction mechanisms at oxide-water interfaces. In: Hochella MF, Jr, White AF, editors. Reviews in mineralogy, vol 23, Mineral-water interface geochemistry. Washington, DC: Mineralogical Society of America. p 309-363.
- Chang H, Healy TW, Matijevic E. 1983. Interactions of metal hydrous oxides with chelating agents, III. Adsorption on spherical colloidal hematite particles. J Colloid Interface Sci 92:469-478.
- Chemical Rubber Company (CRC) Handbook of chemistry and physics. 1977. 58th ed. Boca Raton, FL: CRC Pr. 2179 p.
- Chisholm-Brause CJ, Brown GE, Jr, Parks GA. 1991. In-situ EXAFS study of changes in Co(II) sorption complexes on  $\gamma$ -Al<sub>2</sub>O<sub>3</sub> with increasing sorption densities. In: Hasnain SS, editor. XAFS VI, Sixth international conference on X-ray adsorption fine structure. Chichester, UK: Ellis Horwood. p 263-265.
- Chisholm-Brause CJ, O'Day PA, Brown GE, Jr, Parks GA. 1990. Evidence for multinuclear metal-ion complexes at solid/water interfaces from X-ray adsorption spectroscopy. Nature 348:528-530.
- Davis JA, Hem JD. 1989. The surface chemistry of aluminum oxides and hydroxides. In: Sposito G, editor. The environmental chemistry of aluminum. Boca Raton, FL: CRC Pr. p 185-219.
- Davis JA, James RO, Leckie JO. 1978. Surface ionization and complexation at the oxide/water interface II. Surface properties of amorphous iron oxyhydroxide and adsorption of metal ions. J Colloid Interface Sci 67:90-107.
- Davis JA, Leckie JO. 1978. Surface ionization and complexation at the oxide/water interface I. Computation of electrical double layer properties in simple electrolytes. J Colloid Interface Sci 63:480-499.
- Elliott HA. 1979. The adsorption of copper(II) at the solid-solution interface: effect of complex formation [dissertation]. Newark, DE: Univ of Delaware. 235 p.
- Elliott HA, Huang CP. 1979. The adsorption characteristics of Cu(II) in the presence of chelating agents. J Colloid Interface Sci 70:29-45.
- Felmy AR. 1990. GMIN: a computerized chemical equilibrium model using a constrained minimization of the Gibbs free energy. Report PNL-7281. Richland, WA: Pacific Northwest National Laboratory. 52 p.
- Felmy AR, Girvin DC, Jenne EA. 1984. MINTEQ—A computer program for calculating aqueous geochemical equilibria. EPA 600-3-84-032. Springfield, VA: National Technical Information Service. 187 p.
- Gastuche MC, Herbillon A. 1962. Alumina gels: crystallization in a de-ionized medium. Bull Soc Chem Fr 5:1402-1412.
- Girvin DC, Gassman PL, Bolton H, Jr. 1993. Adsorption of aqueous cobalt ethylenediaminetetraacetate by  $\delta$ -Al<sub>2</sub>O<sub>3</sub>. Soil Sci Soc Am J 57(1):47-57.
- Hayes KF. 1987. Equilibrium spectroscopic and kinetic studies of ion adsorption at the oxide/aqueous interface [dissertation]. Palo Alto, CA: Stanford Univ. 260 p.
- Hayes KF, Leckie JO. 1987. Modeling ionic strength effects on cation adsorption at hydrous oxide/solution interfaces. J Colloid Interface Sci 115:564-572.

- Hayes KF, Papelis C, Leckie JO. 1987. Modeling ionic strength effects on anion adsorption at hydrous oxide/solution interfaces. *J Colloid Interface Sci* 125:717–726.
- Hiemstra T, van Riemsdijk WH, Bruggenwert MGM. 1987. Proton adsorption mechanism at the gibbsite and aluminum oxide solid/solution interface. *Netherlands J of Agric Sci* 35:281–293.
- Hingston FJ, Posner AM, Quirk JP. 1972. Anion adsorption by goethite and gibbsite. I. The role of the proton in determining adsorption envelopes. *J Soil Sci* 23:177–192.
- Hingston FJ, Posner AM, Quirk JP. 1974. Anion adsorption by goethite and gibbsite. II. Desorption of anions from hydrous oxide surfaces. *J Soil Sci* 25:16–26.
- Hsu PH. 1989. Aluminum hydroxides and oxyhydroxides. In: Dickson JB, Weed FB, editors. *Minerals in soil environments*. 2nd ed. Madison, WI: Soil Science Society of America. p 331–378.
- Kavanagh BV, Posner AM, Quirk JP. 1975. Effect of polymer adsorption on properties of the electrical double layer. *Faraday Discuss Chem Soc* 59:242–249.
- Kummert R, Stumm W. 1980. The surface complexation of organic acids on hydrous  $\delta$ - $\text{Al}_2\text{O}_3$ . *J Colloid Interface Sci* 75:373–385.
- Kyle JH, Posner AM, Quirk JP. 1975. Kinetics of isotopic exchange of phosphate adsorbed on gibbsite. *J Soil Sci* 26:32–43.
- Martell AE, Smith RM. 1974. *Critical stability constants*, vol 1: Amino acids. New York: Plenum Pr. 469 p.
- McBride MB. 1985. Influence of glycine on  $\text{Cu}^{2+}$  adsorption by microcrystalline gibbsite and boehmite. *Clays Clay Miner* 33:397–402.
- McKinley JP, Zachara JM, Smith SC, Turner GD. 1995. The influence of uranyl hydrolysis and multiple site-binding reactions on adsorption of U(VI) to montmorillonite. *Clays Clay Miner* 43:586–598.
- Means JL, Alexander CA. 1981. The environmental biogeochemistry of chelating agents and recommendations for the disposal of chelated radioactive wastes. *Nucl Chem Waste Manage* 2:183–196.
- Means JL, Crerar DA, Duguid JO. 1978. Migration of radionuclide wastes: Radionuclide mobilization by complexing agents. *Science* 200:1477–1486.
- Naumov GB, Ryzhenko BN, Khodakovskiy IL. 1974. *Handbook of thermodynamic data*. PB 226 722. Springfield, VA: National Technical Information Service. 286 p.
- Olsen CR, Lowry PD, Lee SY, Larsen IL, Cutshall NH. 1986. Geochemical and environmental processes affecting radionuclide migration from a formerly used seepage trench. *Geochim Cosmochim Acta* 50:593–607.
- Osaki S, Yasuhiro K, Sugihara S, Takashima Y. 1990. Effects of metal ions and organic ligands on the adsorption of Co(II) onto silicagel. *Sci Total Environ* 99:93–103.
- Parfitt RL, Fraser AR, Russell JD, Farmer VC. 1977. Adsorption on hydrous oxides. II Oxalate, benzoate and phosphate on gibbsite. *J Soil Sci* 28:40–47.
- Piciulo PL, Adams JW, Davis MS, Milian LW, Anderson CI. 1986. Release of organic chelating agents from solidified decontamination wastes. NUREG/Cr-4790, BNL-NE-WREG-52014. Washington, DC: US Nuclear Regulatory Commission. 121 p.
- Rabenstein DL, Kula RJ. 1969. Ligand-exchange kinetics and solution equilibria of cadmium, zinc, and lead nitrilotriacetate complexes. *J Am Chem Soc* 91:2492–2503.
- Riley RG, Zachara JM, Wobber FJ. 1992. Chemical contaminants on DOE lands and selection of contaminant mixtures of subsurface science research. DOE/ER-0547T. Washington, DC: US Department of Energy. 77 p.
- Saalfeld N. 1960. Strukturen des Hydrargillitis und der Zwischenstufen beim Entwässern. *Neues Jb Miner Abh* 95:1–87.
- Schindler PW. 1990. Co-adsorption ions and organic ligands: formation of ternary surface complexes. In: Hochella MF, Jr, White AF, editors. *Reviews in mineralogy*, vol 23: Mineral-water interface geochemistry. Washington, DC: Mineralogical Society of America. p 281–307.
- Seyfried MS, Sparks DL, Bar-Tal A, Feigenbaum S. 1989. Kinetics of calcium-magnesium exchange on soil using a stirred-flow reaction chamber. *Soil Sci Soc Am J* 53:406–410.
- Sposito G. 1984. *The surface chemistry of soils*. New York: Oxford Univ Pr. 234 p.
- Szecsody JE, Zachara JM, Bruckhart PL. 1994. Adsorption-dissolution reactions affecting the distribution and stability of Co(II)EDTA in Fe-oxide coated sand. *Environ Sci Technol* 28:1706–1716.
- Toste AP, Lucke RB, Lechner-Fish TJ, Hendren DJ, Myers RB. 1987. Organic analysis of mixed nuclear wastes. In: Post RG, editor. *Waste management '87: proceedings of a symposium on waste management; March 1987; vol 3, Low-level waste*. Tucson, AZ: Univ of Arizona. p 323–329.
- Toste AP, Pahl TR, Lucke RB, Myers RB. 1987. Analysis of complex organic mixtures in nuclear wastes. In: Gray RH, Chess EK, Mellinger PJ, Riley RG, Springer DL, editors. *Health and environmental research on complex organic mixtures. Proceedings of 24th Hanford Life Sciences Symposium: 1985 Oct 20-24; Conference-851027*. Springfield, VA: National Technical Information Service. p 133–150.
- Vuceta J. 1976. Adsorption of Pb(II) and Cu(II) on  $\alpha$ -quartz from aqueous solutions: influence of pH, ionic strength, and complexing ligands [dissertation]. Pasadena, CA: California Inst of Technology. 204 p.
- Westall J. 1982a. FITEQL: a computer program for determination of equilibrium constants from experimental data. Version 1.2. Report 82-01. Corvallis, OR: Department of Chemistry, Oregon State Univ. 98 p.
- Westall J. 1982b. FITEQL: a computer program for determination of equilibrium constants from experimental data. Version 2.0. Report 82-02. Corvallis, OR: Department of Chemistry, Oregon State Univ. 61 p.
- Zachara JM, Smith SC, Kuzel LS. 1994. Adsorption and dissolution of Co-EDTA complex Fe-oxide containing subsurface sands. *Geochim Cosmochim Acta* 59:4825–4844.

(Received 17 January 1995; accepted 14 February 1996; Ms. 2609)